

Get the **Angewandte App**
International Edition

Available on the
App Store

Enjoy Easy Browsing and a New Reading Experience on the iPad

- Keep up to date with the latest articles in Early View.
- Download new weekly issues automatically when they are published.
- Read new or favorite articles anytime, anywhere.



"... France has a long-standing tradition of research and innovation in chemistry, and its chemical industry (ranked fifth in the world) is still a strong pillar of the French economic development ..."

Read more in the Editorial by Alain Fuchs.

Editorial

A. Fuchs* _____ 12632 – 12633

Chemistry in France: A Hotbed for New Schools of Thought

Spotlight on Angewandte's Sister Journals

12652 – 12654

Service



"Chemistry is fun because new findings raise my spirits. When I was eighteen I wanted to be either a mathematician or a chemist. ..."

This and more about Masahiro Miura can be found on page 12656.

Author Profile

Masahiro Miura _____ 12656

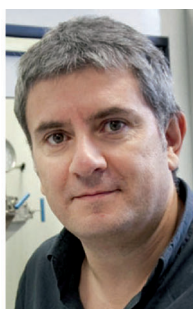
News



N. Martín



J. M. Poblet



E. Peris



P. Ballester

Real Sociedad Española de Química
Prizes 2012 _____ **12657 – 12658**



J. M. Pingarrón



E. Barea



E. J. Cocinero



M. del C. G. López



S. O. Gutiérrez



A. Fürstner



M. Armand



S. Álvarez

Books

Isocyanide Chemistry

Valentine G. Nenajdenko

reviewed by G. C. Tron _____ **12659**

For the USA and Canada:
ANGEWANDTE CHEMIE International Edition (ISSN 1433-7851) is published weekly by Wiley-VCH, PO Box 191161, 69451 Weinheim, Germany. Air freight and mailing in the USA by Publications Expediting Inc., 200 Meacham Ave., Elmont, NY 11003. Periodicals

postage paid at Jamaica, NY 11431. US POSTMASTER: send address changes to *Angewandte Chemie*, Journal Customer Services, John Wiley & Sons Inc., 350 Main St., Malden, MA 02148-5020. Annual subscription price for institutions: US\$ 11.738/10.206 (valid for print and electronic / print or electronic delivery); for

individuals who are personal members of a national chemical society prices are available on request. Postage and handling charges included. All prices are subject to local VAT/sales tax.

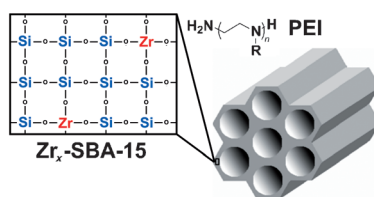
Highlights

CO₂ Capture

J. P. Sculley, H.-C. Zhou* 12660 – 12661

Enhancing Amine-Supported Materials for Ambient Air Capture

Worth the wait: A new variable, zirconium content, has been added to the already complex amine-supported porous silica systems used for CO₂ capture. SBA-15 incorporating Zr ions and loaded with poly(ethyleneimine) was exposed to simulated flue gas (10% CO₂) and ambient air (400 ppm CO₂). Not only was the performance of the Zr-doped material significantly better than that of the pristine system, it also displayed improved desorption kinetics.

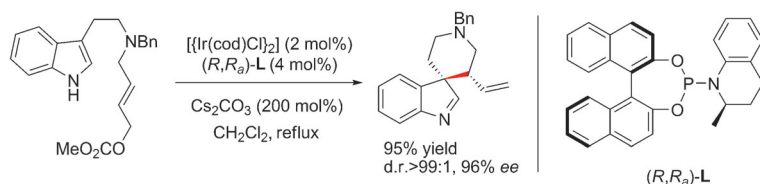


Reviews

Asymmetric Catalysis

C.-X. Zhuo, W. Zhang,*
S.-L. You* 12662 – 12686

Catalytic Asymmetric Dearomatization Reactions



Breaking up the party: Arenes can be transformed efficiently into enantiomerically enriched, versatile ring systems by catalytic asymmetric dearomatization reactions. Known reaction types include oxidative dearomatization, dearomatiza-

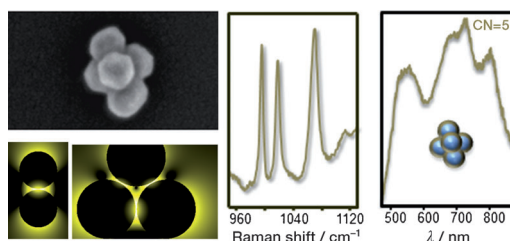
tion by Diels–Alder reactions, alkylative dearomatization of electron-rich arenes, transition-metal-catalyzed dearomatization reactions (see example), and cascade reaction sequences involving asymmetric dearomatization as the key step.

Communications

Nanoparticle Clusters

N. Pazos-Perez, C. S. Wagner,
J. M. Romo-Herrera, L. M. Liz-Marzán,
F. J. García de Abajo,* A. Wittemann,*
A. Fery,*
R. A. Alvarez-Puebla* 12688 – 12693

Organized Plasmonic Clusters with High Coordination Number and Extraordinary Enhancement in Surface-Enhanced Raman Scattering (SERS)



Highly symmetric gold nanoparticle clusters with coordination numbers up to seven were produced by using coating with block copolymers. The resulting

clusters were separated by density gradient centrifugation and characterized by using SEM and optical spectroscopy (see picture).

Frontispiece

The German Chemical Society (GDCh) invites you to:



Angewandte Anniversary Symposium

GDCh
Eine Zeitschrift der Gesellschaft Deutscher Chemiker

Tuesday, March 12, 2013

Henry Ford Building / FU Berlin

Speakers



Carolyn R.
Bertozzi



François
Diederich



Alois
Fürstner



Roald Hoffmann
(Nobel Prize 1981)



Susumu
Kitagawa



Jean-Marie Lehn
(Nobel Prize 1987)



E.W. "Bert"
Meijer



Frank
Schirrmacher
(Publisher, FAZ)



Robert
Schlögl



George M.
Whitesides



Ahmed Zewail
(Nobel Prize 1999)

More information:

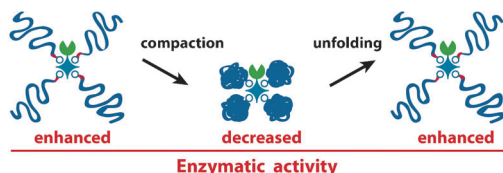


angewandte.org/symposium



 **WILEY-VCH**


GESELLSCHAFT
DEUTSCHER CHEMIKER



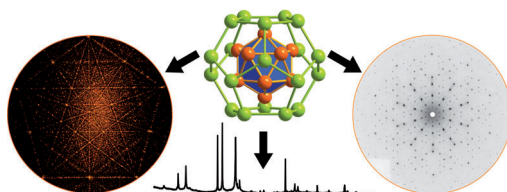
A giant DNA leap for enzyme-kind: Giant DNA–protein multibranch conjugates were shown to be composed of a single β -lactamase enzyme (green, see scheme) conjugated to up to four 48.5 kbp lambda

phage DNA branches (blue lines). The conjugation of giant DNA induces a two- to fourfold enhancement of the enzymatic activity, which is modulated by changes in the higher-order DNA structure.

DNA–Enzyme Conjugates

S. Rudiuk, A. Venancio-Marques,
D. Baigl* 12694 – 12698

Enhancement and Modulation of Enzymatic Activity through Higher-Order Structural Changes of Giant DNA–Protein Multibranch Conjugates



Golden opportunity: $\text{Na}_{13}\text{Au}_{12}\text{Ga}_{15}$ is the first Na-containing, thermodynamically stable quasicrystal and was discovered during systematic exploration of the polar intermetallic Na–Au–Ga system. Its electron-to-atom ratio, 1.75, is extremely low

for Bergman-type icosahedral phases, but it is the substantial Au content that allows Hume–Rothery stabilization and promotes novel Na–Au polar-covalent interactions, which stabilize the icosahedral phase.

Intermetallic Phases

V. Smetana, Q. Lin, D. K. Pratt,
A. Kreysig, M. Ramazanoglu,
J. D. Corbett, A. I. Goldman,
G. J. Miller* 12699 – 12702

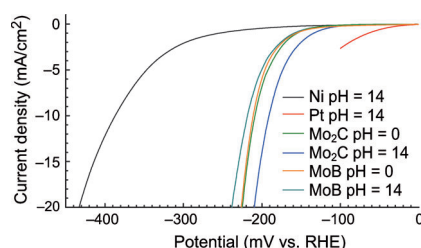
A Sodium-Containing Quasicrystal: Using Gold To Enhance Sodium's Covalency in Intermetallic Compounds



Back Cover



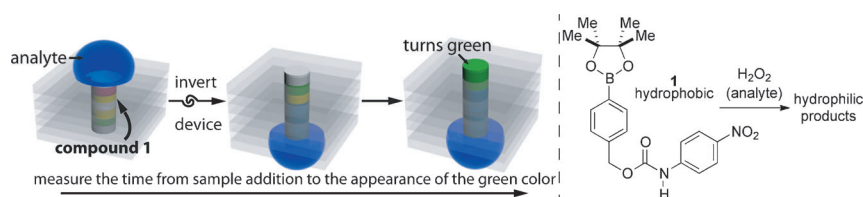
Getting the hydrogen out: Molybdenum boride (MoB) and carbide (Mo_2C) are excellent catalysts for electrochemical hydrogen evolution at both pH 0 and pH 14.



Water Splitting

H. Vrubel, X. Hu* 12703 – 12706

Molybdenum Boride and Carbide Catalyze Hydrogen Evolution in both Acidic and Basic Solutions



A matter of time: Two quantitative assays are presented that require only measurements of time and the ability to see and/or count to quantify the presence of a specific analyte. The strategies rely on specific changes in wetting properties of paper

when a hydrophobic detection reagent (compound 1) reacts with a desired analyte to produce hydrophilic products. This change in wetting properties enables selective and quantitative detection of the analyte.

Assay Development

G. G. Lewis, M. J. DiTucci,
S. T. Phillips* 12707 – 12710

Quantifying Analytes in Paper-Based Microfluidic Devices Without Using External Electronic Readers

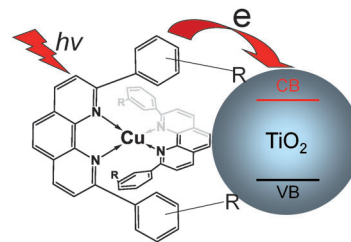


Photosensitizers

J. Huang, O. Buyukcakir, M. W. Mara,
A. Coskun, N. M. Dimitrijevic, G. Barin,
O. Kokhan, A. B. Stickrath, R. Ruppert,
D. M. Tiede, J. F. Stoddart, J.-P. Sauvage,*
L. X. Chen* _____ **12711 – 12715**



Cu complexes as photosensitizers: Photoinduced charge-transfer dynamics from a copper(I) diimine complex to TiO₂ nanoparticles were investigated by combining multiple time-resolved spectroscopic methods. An efficient and ultrafast electron transfer process from the singlet MLCT state was discovered as a result of structural control owing to the flattening of the tetrahedral geometry in the complex and the bulky groups in the ligands.

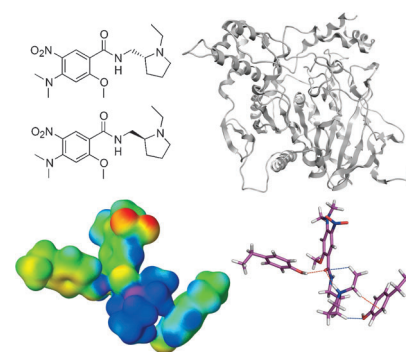


Molecular Recognition

L. Berg, M. S. Niemiec, W. Qian,
C. D. Andersson, P. Wittung-Stafshede,
F. Ekström,*
A. Linusson* **12716–12720**



Take a closer look: Unexpectedly, a pair of enantiomeric ligands proved to have similar binding affinities for acetylcholinesterase. Further studies indicated that the enantiomers exhibit different thermodynamic profiles. Analyses of the non-covalent interactions in the protein–ligand complexes revealed that these differences are partly due to nonclassical hydrogen bonds between the ligands and aromatic side chains of the protein.

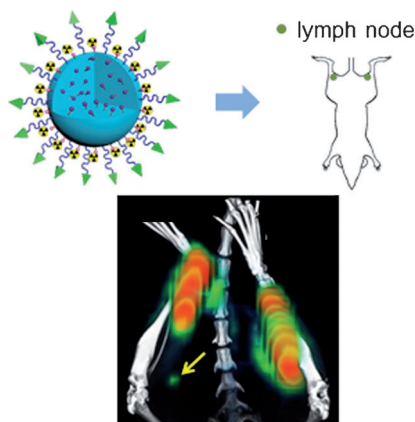


PET/NIR Imaging

L. Tang, X. Yang, L. W. Dobrucki,
I. Chaudhury, Q. Yin, C. Yao, S. Lezmi,
W. G. Helferich,* T. M. Fan,*
J. Cheng* **12721–12726**



A dual-modal imaging probe based on size-controlled silica nanoconjugates was synthesized for targeted imaging of lymph nodes by means of both PET and near infrared fluorescence techniques. 20 nm nanoconjugates (see scheme) functionalized with an aptamer (green triangles) that targets 4T1 breast cancer cells improved the detection efficiency of sentinel lymph nodes with metastatic tumors.

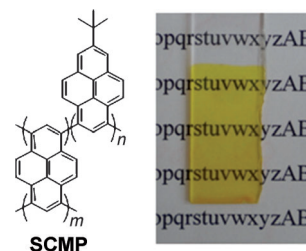


Porous Polymers

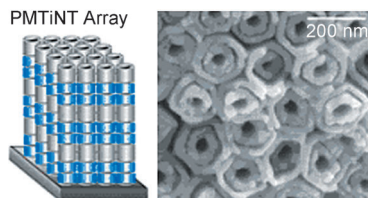
G. Cheng, T. Hasell, A. Trewin,
D. J. Adams,
A. I. Cooper* _____ **12727–12731**



Soluble and porous: Soluble conjugated microporous polymers (SCMPs) can be prepared by synthesizing discrete hyper-branched molecules. The materials can be cast from solution as thin films (see picture), suggesting a range of processing options that are not available for insoluble CMP networks. Soluble, conjugated dendrimers are porous and give insight into the structural origin of microporosity.



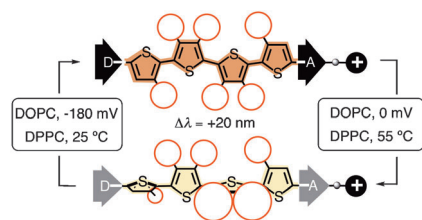
Cu–Pt bimetallic shells supported on a double-walled TiO₂ nanotube (PMTiNT) array are efficient photocatalysts for the room-temperature conversion of CO₂ into light hydrocarbons, such as CH₄, C₂H₄, and C₂H₆. When Cu_{0.33}–Pt_{0.67}/PMTiNT was used for the photoreduction of diluted CO₂ (1 % in N₂), an average hydrocarbon production rate of 3.7 mL g^{−1} h^{−1} or 6.1 mmol m^{−2} h^{−1} was realized under AM1.5 one-sun illumination.



CO₂ Photoreduction

X. Zhang, F. Han, B. Shi, S. Farsinezhad, G. P. Dechaine, K. Shankar* 12732–12735

Photocatalytic Conversion of Diluted CO₂ into Light Hydrocarbons Using Periodically Modulated Multiwalled Nanotube Arrays



Lessons from lobster coloration and the chemistry of vision suggested an approach to responsive fluorescent probes that can sense membrane potential, fluidity, and tension. Fluorophore deplanarization by lateral crowding along the scaffold (red circles) and fluorophore polarization by terminal donors (D), acceptors (A), and charges (+) are coupled to provide such membrane probes, as studies with unilamellar vesicles of phospholipids (DOPC, DPPC) show.

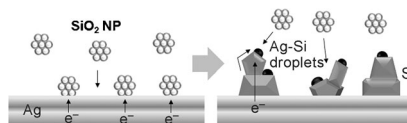
Fluorescent Probes

A. Fin, A. Vargas Jentzsch, N. Sakai, S. Matile* 12736–12739

Oligothiophene Amphiphiles as Planarizable and Polarizable Fluorescent Membrane Probes



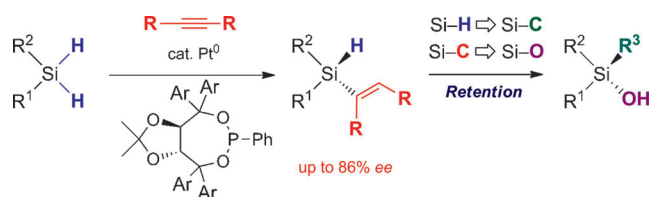
Silicon for solar cells: Relatively pure, polycrystalline, and photoactive silicon was directly obtained from silicon dioxide nanoparticles (NP) by electrodeposition in molten CaCl₂ salt on a silver electrode (see picture). This process is based on the formation of liquid droplets of a silver–silicon eutectic alloy and the continuous reduction of SiO₂ to silicon. The deposited silicon shows a p-type behavior in photoelectrochemical measurements.



Electrochemistry

S. K. Cho, F.-R. F. Fan, A. J. Bard* 12740–12744

Electrodeposition of Crystalline and Photoactive Silicon Directly from Silicon Dioxide Nanoparticles in Molten CaCl₂



Asymmetric silanes: A synthesis of non-racemic alkenylhydrosilanes has been developed based on the desymmetrization of a dihydrosilane through alkenylation with an alkyne using an asymmetric catalyst. The alkenylhydrosilane product

can be used as a versatile chiral building block for other functionalized nonracemic silanes through the stereoselective conversion of its hydride and/or alkenyl moiety.

Chiral Silanes

K. Igawa, D. Yoshihiro, N. Ichikawa, N. Kokan, K. Tomooka* 12745–12748

Catalytic Enantioselective Synthesis of Alkenylhydrosilanes

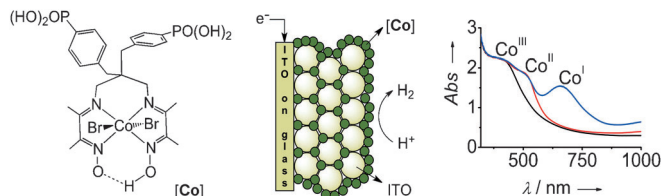


Hybrid Materials

N. M. Muresan, J. Willkomm, D. Mersch,
Y. Vaynzof, E. Reisner* — 12749–12753



Immobilization of a Molecular
Cobaloxime Catalyst for Hydrogen
Evolution on a Mesoporous Metal Oxide
Electrode



Energizing Cobalt on a 3D Electrode: An optically transparent mesoporous ITO film was derivatized with the novel proton reducing cobalt catalyst [Co]. The hybrid electrode showed high current densities,

and spectroelectrochemical studies and extensive surface characterization demonstrate that the immobilized molecular catalyst remained intact on the electrode when applying a low potential.

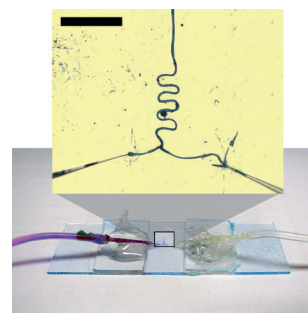
Polyoxometalates

G. J. T. Cooper, R. W. Bowman,
E. P. Magennis, F. Fernandez-Trillo,
C. Alexander, M. J. Padgett,*
L. Cronin* — 12754–12758



Directed Assembly of Inorganic
Polyoxometalate-based Micrometer-Scale
Tubular Architectures by Using Optical
Control

Go with the flow: Laser-induced flow patterns are used to direct the self-assembly of dissolved inorganic polyoxometalate clusters into robust, hollow tubular networks and micro-materials (see picture; scale bar: 500 μm) in real time. The hollow nature of these materials can be exploited to develop devices in which the self-assembled tubes act as microscopic flow channels.



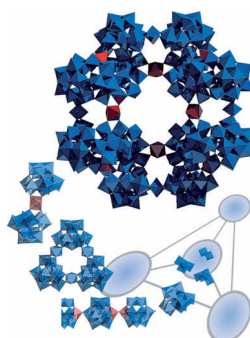
Front Cover

Polyoxometalates

A. R. de la Oliva, V. Sans, H. N. Miras,
J. Yan, H. Zang, C. J. Richmond,
D.-L. Long, L. Cronin* — 12759–12762



Assembly of a Gigantic Polyoxometalate
Cluster {W₂₀₀Co₈O₆₆₀} in a Networked
Reactor System



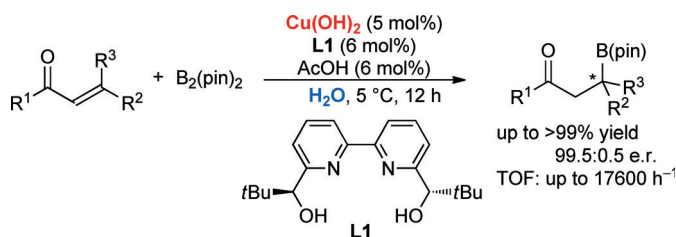
A giant leap: A networked reactor system was used for the first time for the discovery and synthesis of new polyoxometalates, including the gigantic title system (see picture; Co red, W blue). The system comprises of three reactors connected in a triangular array with a central triply connected reactor. This system was used to screen multiple one-pot reactions and reaction variables for the automated syntheses of polyoxometalates.

Asymmetric Catalysis

S. Kobayashi,* P. Xu, T. Endo, M. Ueno,
T. Kitano — 12763–12766

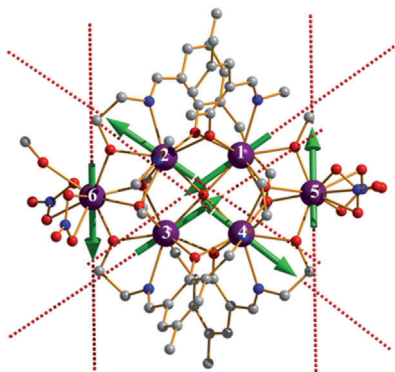


Chiral Copper(II)-Catalyzed
Enantioselective Boron Conjugate
Additions to α,β-Unsaturated Carbonyl
Compounds in Water



Copper pins on the boron: The enantioselective 1,4-addition of diboron to α,β-unsaturated compounds proceeds smoothly in the presence of catalytic amounts of Cu(OH)₂ and chiral 2,2'-bipyridine ligand in water. A wide sub-

strate scope of α,β-unsaturated carbonyl compounds, including acyclic, cyclic, and β,β-disubstituted enones, α,β-unsaturated esters, amides, and a nitrile, has been shown.

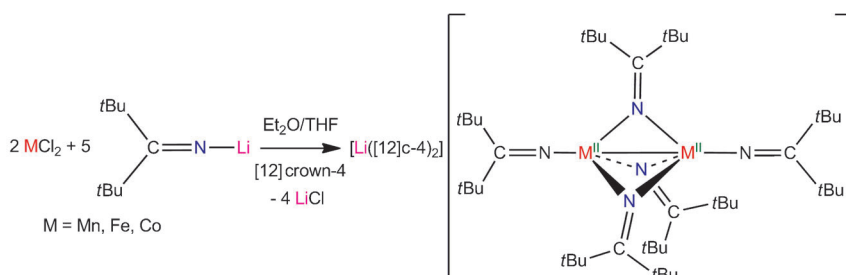


A hexanuclear dysprosium(III) compound constructed by two Dy_3 triangles in an edge-to-edge arrangement perfectly retains a nonmagnetic ground state and single-molecular-magnet behavior. Such an arrangement and the strong couplings over a $\mu_4\text{-O}^{2-}$ ion stabilize a similar arrangement of toroidal moments in the ground state, thus maximizing the toroidal moment of the complex. (Picture: Dy purple, C gray, N blue, O red.)

Single-Molecule Magnets

S. Y. Lin, W. Wernsdorfer, L. Ungur, A. K. Powell, Y. N. Guo, J. Tang,* L. Zhao, L. F. Chibotaru,*
H. J. Zhang* — 12767–12771

Coupling Dy_3 Triangles to Maximize the Toroidal Moment



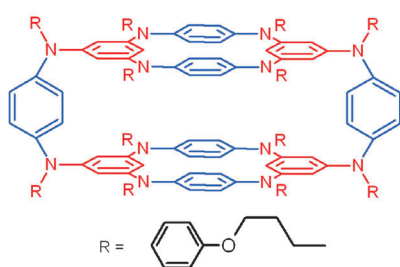
Bond, metal–metal bond: Addition of 2.5 equiv of $\text{Li}(\text{N}=\text{CtBu}_2)$ to MCl_2 ($\text{M} = \text{Mn, Fe, and Co}$), followed by addition of $[12]\text{crown-4}$, results in formation of $[\text{Li}([12]\text{crown-4})_2][\text{M}_2(\text{N}=\text{CtBu}_2)_5]$ in good yields. These complexes exhibit short

$\text{M}-\text{M}$ distances and strong magnetic communication between metal centers, thus demonstrating that ketimides are viable co-ligands for promoting metal–metal bonding.

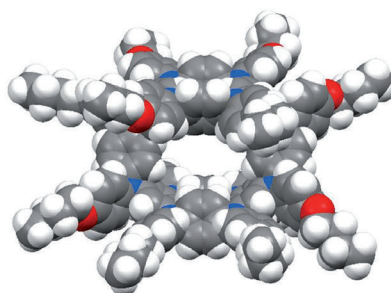
Metal Ketimides

R. A. Lewis, S. Morochnik, A. Chapovetsky, G. Wu, T. W. Hayton* — 12772–12775

Synthesis and Characterization of $[\text{M}_2(\text{N}=\text{CtBu}_2)_5]^-$ ($\text{M} = \text{Mn, Fe, Co}$): Metal Ketimide Complexes with Strong Metal–Metal Interactions



Spin doctor: The polymacrocyclic oligoarylamine in the picture serves as a multi-spin source owing to its multi-electron redox activity. As a result of its pseudobeltane structure and *para*-phenylene-diamine bridges, the radical cation can



convert between two sideslipped structures with a windshield-wiper-like motion. In contrast, the tetraazacyclophane units are rigid components in the polymacrocyclic.

Cyclophanes

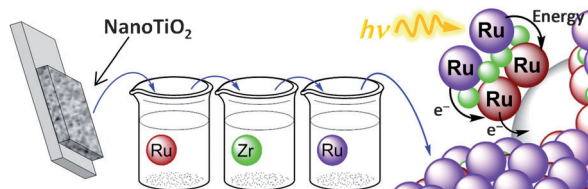
D. Sakamaki, A. Ito,* K. Furukawa, T. Kato, M. Shiro, K. Tanaka* — 12776–12781

A Polymacrocyclic Oligoarylamine with a Pseudobeltane Motif: Towards a Cylindrical Multispin System



Electron Transfer

K. Hanson, D. A. Torelli, A. K. Vannucci,
M. K. Brennaman, H. Luo, L. Alibabaei,
W. Song, D. L. Ashford, M. R. Norris,
C. R. K. Glasson, J. J. Concepcion,
T. J. Meyer* — 12782 – 12785

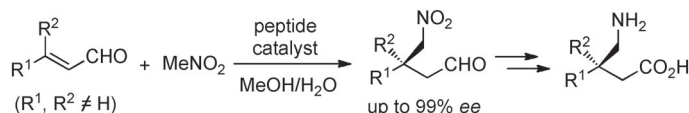


Simple assembly: A “layer-by-layer” deposition of functionalized dyes/catalysts on the surfaces of nanocrystalline oxides is introduced. The strategy is general and offers considerable flexibility based on

phosphonate- or carboxylate-binding groups with Zr^{IV} as bridging ions. The resulting bilayer structures are capable of supporting rapid intra-layer energy and electron transfer (see picture).

Peptide Catalysis

K. Akagawa, K. Kudo* — 12786 – 12789



peptide catalyst = **Pro-D-Pro-Aib-(Trp)₂-(Leu)₆**

Construction of an All-Carbon Quaternary Stereocenter by the Peptide-Catalyzed Asymmetric Michael Addition of Nitromethane to β -Disubstituted α,β -Unsaturated Aldehydes

Pepping up Michael: An asymmetric Michael addition of nitromethane to β -disubstituted α,β -unsaturated aldehydes was realized by a resin-supported peptide catalyst. Whereas the use of a low-

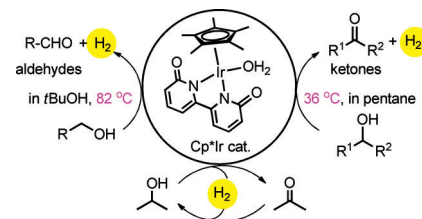
molecular-weight catalyst resulted in poor yields, the peptide effectively promoted the reaction in aqueous media with high enantioselectivity.

Dehydrogenation

R. Kawahara, K. Fujita,*
R. Yamaguchi* — 12790 – 12794

Cooperative Catalysis by Iridium Complexes with a Bipyridonate Ligand: Versatile Dehydrogenative Oxidation of Alcohols and Reversible Dehydrogenation–Hydrogenation between 2-Propanol and Acetone

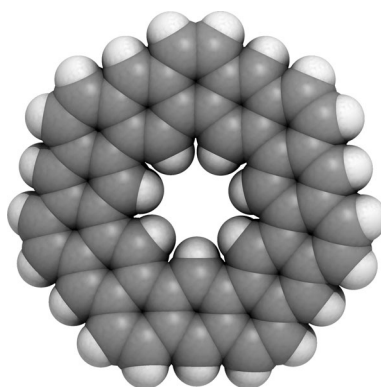
Going into reverse: An efficient and versatile catalytic system for the dehydrogenative oxidation of alcohols under extremely mild conditions has been developed using a Cp^{*}Ir complex with bipyridonate ligand as catalyst (see scheme, Cp^{*} = pentamethylcyclopentadienyl). Reversible and repetitive transformation between 2-propanol and acetone by catalytic dehydrogenation–hydrogenation is also achieved.



Kekulene

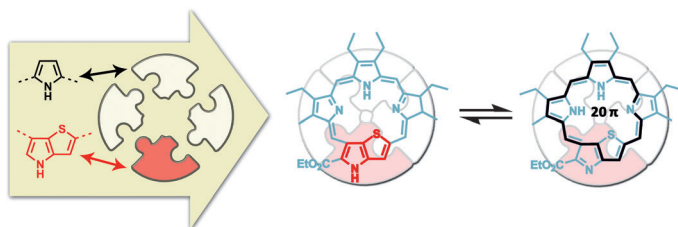
B. Kumar, R. L. Viboh, M. C. Bonifacio,
W. B. Thompson, J. C. Buttrick,
B. C. Westlake, M.-S. Kim, R. W. Zoellner,
S. A. Varganov, P. Mörschel, J. Teteruk,
M. U. Schmidt,
B. T. King* — 12795 – 12800

Septulene: The Heptagonal Homologue of Kekulene



A family likeness: The seven-sided homologue of kekulene, septulene (see structure), has been synthesized in seven steps by ring-closing metathesis. Its properties (spectroscopic and structural) are strikingly similar to those of kekulene despite its sevenfold symmetry and resulting non-alternant structure. The chair-type conformation in the crystal arises from packing forces. Septulene is probably a free pseudorotor in the gas phase.

Inside Back Cover



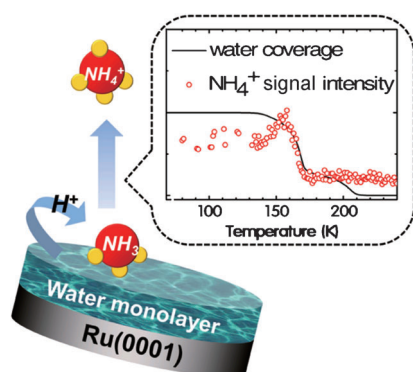
Easy as π : A stable nonaromatic heteroporphyrin bearing a thienopyrrole moiety has been prepared. The nonaromatic nature of this compound is clearly evident based on UV/Vis absorption, ^1H NMR spectroscopy, and theoretical calculations.

Single-crystal X-ray analysis demonstrates that the molecule adopts a planar conformation with clear alternation in the C–C bond lengths around the periphery of the macrocycle.

Porphyrinoids

Y. Chang, H. Chen, Z. Zhou, Y. Zhang,
C. Schütt, R. Herges,
Z. Shen* 12801–12805

A 20 π -Electron Heteroporphyrin
Containing a Thienopyrrole Unit

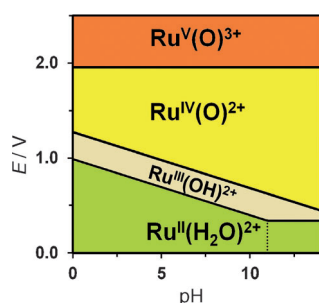


Acidic water: The first monolayer of water on a Ru(0001) surface is anomalously acidic compared to bulk water, according to infrared and mass spectroscopic investigations of the water layer using ammonia as a probe for surface acidity. The observation suggests that acid–base chemistry may be quite different at the water–metal interfaces than in aqueous solution.

Water–Solid Interfaces

Y. Kim, E.-s. Moon, S. Shin,
H. Kang* 12806–12809

Acidic Water Monolayer on
Ruthenium(0001)

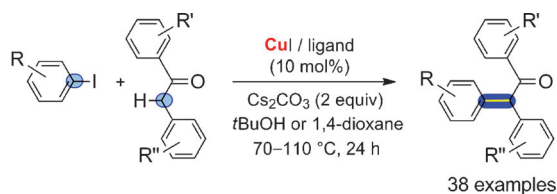


We can do better! The new density functionals M11-L and M11 and the SMD implicit solvation model were used to predict reduction potential–pH equilibrium diagrams (see example) for two ruthenium-based water-oxidation catalysts and their derivatives in aqueous solution. The observed improved accuracy for transition-metal complexes opens new opportunities for the use of theory in the understanding and design of catalysts containing transition metals.

Computational Electrochemistry

A. V. Marenich, A. Majumdar, M. Lenz,
C. J. Cramer,*
D. G. Truhlar* 12810–12814

Construction of Pourbaix Diagrams for
Ruthenium-Based Water-Oxidation
Catalysts by Density Functional Theory



No activation needed: The first efficient method for direct α -arylation of non-activated or non-protected family of enolizable ketones with simple aryl iodides employs a catalytic copper system. The method shows potential for the easy and

step-economical synthesis of tamoxifen, the most commonly administrated drug for the management of breast cancer. R, R', R'' = electron-donating or electron-withdrawing groups.



Synthetic Methods

G. Danoun, A. Tlili, F. Monnier,
M. Taillefer* 12815–12819

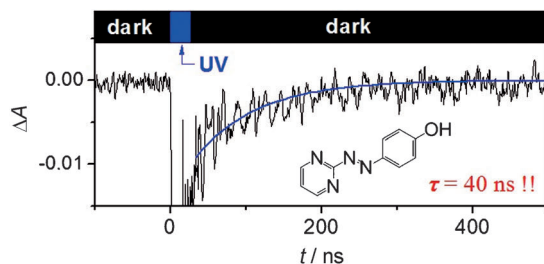
Direct Copper-Catalyzed α -Arylation of
Benzyl Phenyl Ketones with Aryl Iodides:
Route towards Tamoxifen



Fast Photoswitches

J. Garcia-Amorós, M. Díaz-Lobo,
S. Nonell, D. Velasco* — 12820–12823

Fastest Thermal Isomerization of an Azobenzene for Nanosecond Photoswitching Applications under Physiological Conditions



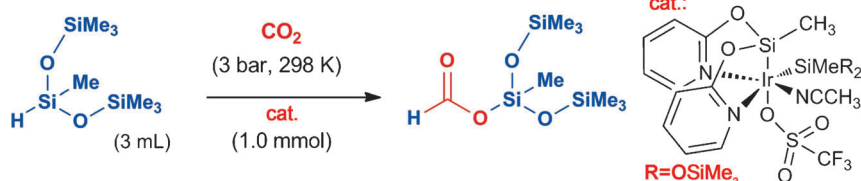
E. coli

When speed is of the essence: After photoisomerization to its metastable *cis* form, an azo dye must undergo fast thermal isomerization back to the *trans* form to be suitable for real-time information transmission. The azopyrimidine

shown has a relaxation time (τ) of just 40 ns under physiological conditions, as well as high biocompatibility, as determined by *Escherichia coli* growth in its presence (see picture).

CO₂ Hydrosilylation

R. Lalrempuia, M. Iglesias, V. Polo,
P. J. Sanz Miguel,
F. J. Fernández-Alvarez,*
J. J. Pérez-Torrente,
L. A. Oro* — 12824–12827



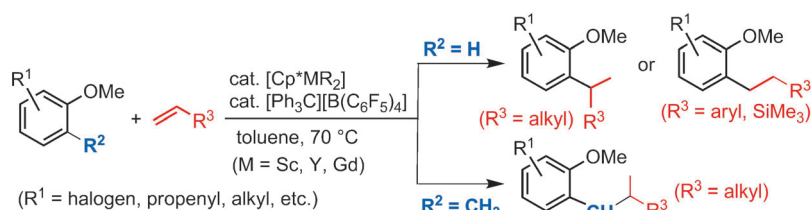
CO₂ as feedstock: An air- and moisture-stable iridium(III) catalyst effectively promotes the hydrosilylation of CO₂. This reaction leads to silyl formate in a highly

selective manner and proceeds efficiently under mild conditions, most likely by an outer-sphere mechanism, as suggested by theoretical calculations.

C–H Alkylation

J. Oyamada, Z. Hou* — 12828–12832

Regioselective C–H Alkylation of Anisoles with Olefins Catalyzed by Cationic Half-Sandwich Rare Earth Alkyl Complexes



A half sandwich helping: Cationic rare-earth alkyl species generated from half-sandwich rare-earth dialkyl complexes and [Ph₃C][B(C₆F₅)₄] can serve as unique catalysts for the C–H regioselective alkylation

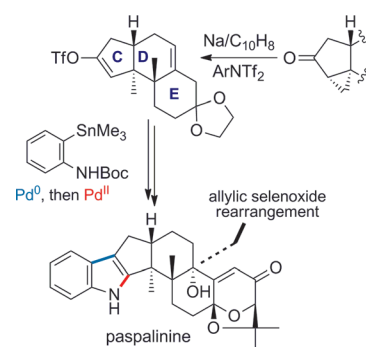
of anisoles with alkenes. The reaction affords either *ortho*-monoalkylated derivatives or products substituted at the benzylic position, depending on the substrate chosen.

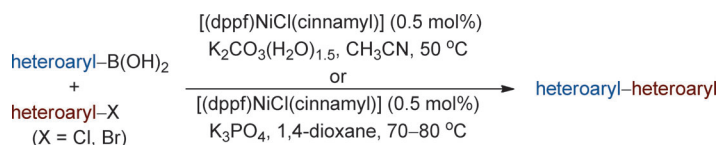
Natural Product Synthesis

M. Enomoto, A. Morita,
S. Kuwahara* — 12833–12836

Total Synthesis of the Tremorgenic Indole Diterpene Paspalinine

Succinct and stereoselective: A high-yielding two-step indole ring installation comprising the Stille cross-coupling and a Pd^{II}-mediated oxidative heterocyclization was exploited in a concise total synthesis of paspalinine. The *trans-anti-trans* CDE fused ring system of the heptacyclic natural product was established highly stereoselectively through hydroxy-directed cyclopropanation and allylic selenoxide rearrangement.





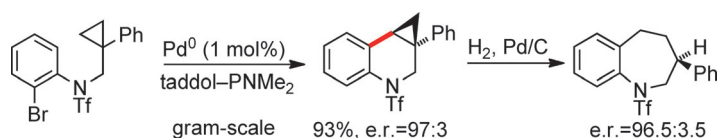
One for all: The coupling of a range of nitrogen- and sulfur-containing heteroaryl halides with five-membered nitrogen-, oxygen-, and sulfur-containing heteroaryl boronic acids were achieved in high yields with only 0.5 mol% of the single-component

nickel precatalyst [(dppf)NiCl(cinnamyl)] (dppf = 1,1'-bis(diphenylphosphanyl)ferrocene). The reaction demonstrates good functional group compatibility, and is easily conducted on a large scale without a dry box.

Heterobiaryl Cross-Coupling

S. Ge, J. F. Hartwig* — 12837 – 12841

Highly Reactive, Single-Component Nickel Catalyst Precursor for Suzuki–Miyaura Cross-Coupling of Heteroaryl Boronic Acids with Heteroaryl Halides



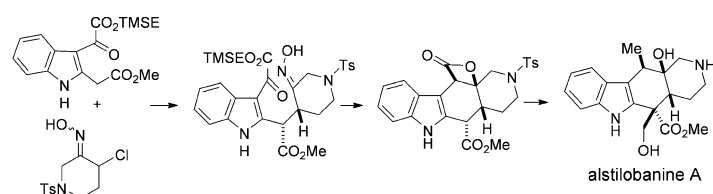
Activated: The title reaction proceeds efficiently with 1 mol% of palladium and gives tetrahydroquinolines in excellent enantioselectivities (see scheme). The enantiodiscriminating concerted metalation–deprotonation step occurs via a rare

seven-membered palladacycle. The cyclopropyl-substituted tetrahydroquinolines can be regioselectively and enantiospecifically reduced to chiral tetrahydrobenzazepines.

C–H Activation

T. Saget, N. Cramer* — 12842 – 12845

Palladium(0)-Catalyzed Enantioselective C–H Arylation of Cyclopropanes: Efficient Access to Functionalized Tetrahydroquinolines



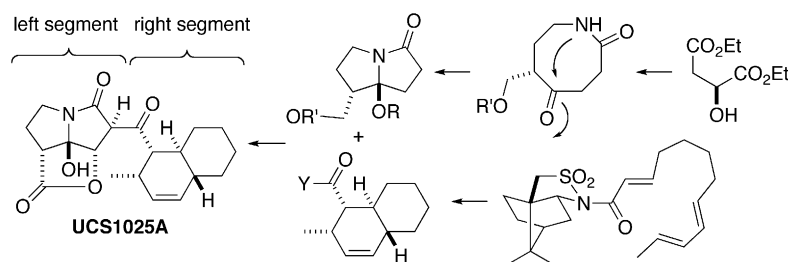
Tetracyclic monoterpene alkaloid alstilobanine A was obtained in racemic form. The pivotal steps of the total synthesis are a novel conjugate addition of an ester enolate with a nitrosoalkene, as well as

a formal [2+2] intramolecular cycloaddition leading to a β -lactone to generate the requisite *cis*-fused 2-azadecalin moiety of the alkaloid. TMSE = trimethylsilylethoxy, Ts = 4-toluenesulfonyl.

Natural Product Synthesis

Y. Feng, M. M. Majireck, S. M. Weinreb* — 12846 – 12849

Total Synthesis of the Unusual Monoterpenoid Indole Alkaloid (\pm)-Alstilobanine A



Under control: A stereocontrolled total synthesis of (+)-UCS1025A, a potent telomerase inhibitor, was achieved. The synthesis features an intramolecular Diels–Alder reaction, a tandem Stau-

dinger/aza-Wittig reaction, and stereoselective construction of the hemiaminal moiety facilitated by neighboring-group participation.

Natural Product

K. Uchida, T. Ogawa, Y. Yasuda, H. Mimura, T. Fujimoto, T. Fukuyama, T. Wakimoto, T. Asakawa, Y. Hamashima, T. Kan* — 12850 – 12853

Stereocontrolled Total Synthesis of (+)-UCS1025A

Multicomponent Oxide Catalysts

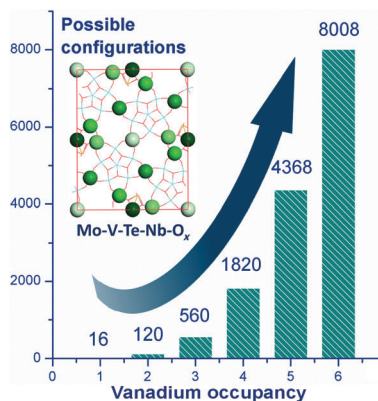
G. Fu, X. Xu, P. Sautet* — 12854–12858



Vanadium Distribution in Four-Component Mo-V-Te-Nb Mixed-Oxide Catalysts from First Principles: How to Explore the Numerous Configurations?



Inside Cover



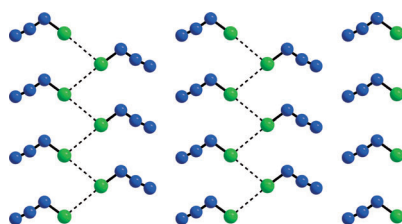
A V V good idea: The V occupancy (shown as a scale of green in the picture) and V–V pair probability in a Mo-V-Te-Nb mixed oxide were determined by weighted average over all possible (up to 8000) configurations on the basis of estimated DFT energies, which agreed well with those obtained by full optimization ($R^2 > 0.94$, maximum error below 0.05 eV). This rapid approach provided insight into the origin of the catalytic activity of these solids.

Halogen Azides

B. Lyhs, D. Bläser, C. Wölper, S. Schulz,*
G. Jansen — 12859–12863



A Comparison of the Solid-State Structures of Halogen Azides XN_3 ($\text{X} = \text{Cl}, \text{Br}, \text{I}$)



Delicate crystals: ClN_3 adopts a polymeric structure in the solid state (see picture; N blue, Cl green) with short intermolecular $\text{Cl}\cdots\text{Cl}$ distances, as was observed for the elemental halogens.

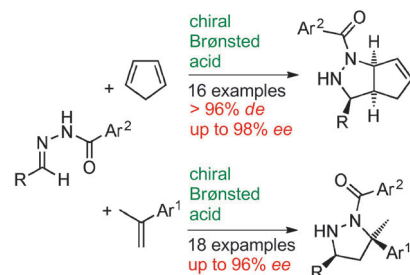
Organocatalysis

M. Rueping,* M. S. Maji, H. B. Küçük,
I. Atodiresei — 12864–12868



Asymmetric Brønsted Acid Catalyzed Cycloadditions—Efficient Enantioselective Synthesis of Pyrazolidines, Pyrazolines, and 1,3-Diamines from *N*-Acyl Hydrazones and Alkenes

A general, metal-free, highly enantioselective Brønsted acid catalyzed [3+2] cycloaddition between hydrazones and alkenes has been developed that affords pyrazolidine derivatives (see scheme). The resulting optically active pyrazolidines can undergo many chemical transformations which allow, for example, the enantioselective synthesis of valuable pyrazolines and 1,3-diamines.



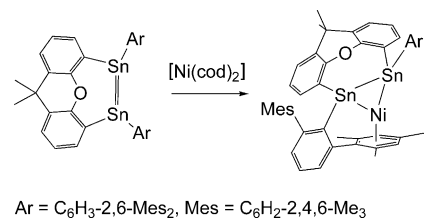
Coordination Chemistry

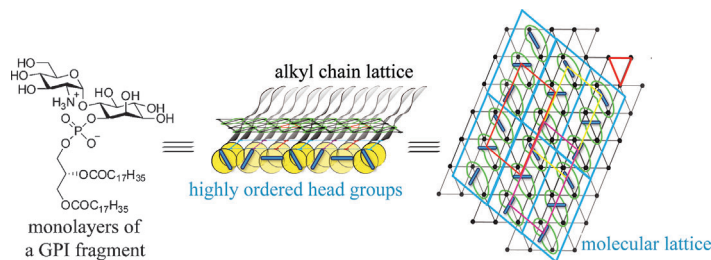
J. Henning,
L. Wesemann* — 12869–12873



Side-On Coordinated Distannene: An Unprecedented Nickel(0) Complex

η^2 -coordination of a Sn–Sn bond: An intramolecular distannene was synthesized in a straightforward fashion from 4,5-dithio-9,9-dimethylxanthene. This compound reacts with $[\text{Ni}(\text{cod})_2]$ to form a Ni^0 complex with an unprecedented Sn_2Ni triangle (see scheme; cod = 1,5-cyclooctadiene).





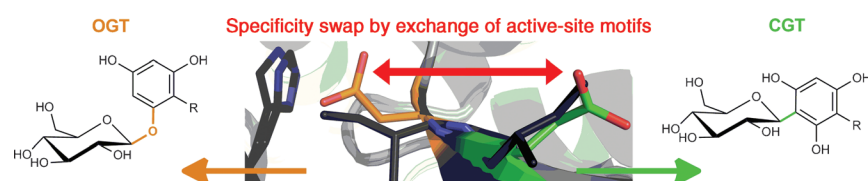
Heads and tails: GPI glycolipid monolayers on the air/liquid interface are characterized by the ordering of entire molecules, as observed by grazing-incidence X-ray diffraction. Strong hydrogen bond-

ing interactions are responsible for ordering of the head groups to form supercells. These forces are likely to be the key to the interactions of GPI-anchored proteins and/or GPIs in cell membranes.

Glycophospholipid Monolayers

C. Stefaniu,* I. Vilotijevic, M. Santer,
D. Varón Silva, G. Brezesinski,
P. H. Seeberger* — 12874–12878

Subgel Phase Structure in Monolayers of
Glycosylphosphatidylinositol Glycolipids



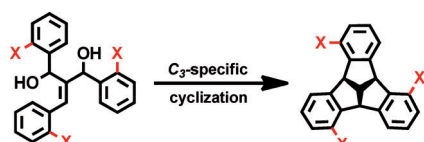
Mechanistic implications: Distinct active-site motifs in plant aryl glucosyltransferases of the GT-1 family differentiate between C- and O-glycosylation activity on a phloretin acceptor. In the implicated protein design principle the exchange of

active-site motifs results in reversible switch between C/O-glycoside specificity. The proposed mechanism of the C-glycosyltransferase involves direct nucleophilic displacement at the anomeric carbon.

Enzyme Mechanisms

A. Gutmann,
B. Nidetzky* — 12879–12883

Switching between O- and C-Glycosyl-
transferase through Exchange of Active-
Site Motifs

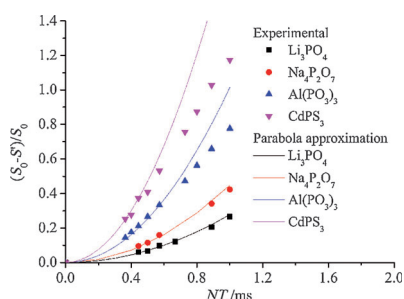


Fusing rings: A new synthesis of the bowl-shaped hydrocarbon tribenzotriquinacene is presented (see scheme). The synthesis allows easy access to *ortho*-functionalized and C₃-chiral derivatives that are attractive for supramolecular chemistry and asymmetric catalysis.

Bowl-Shaped Molecules

G. Markopoulos, L. Henneicke, J. Shen,
Y. Okamoto, P. G. Jones,
H. Hopf* — 12884–12887

Tribenzotriquinacene: A Versatile
Synthesis and C₃-Chiral Platforms



In a new solid-state NMR method
a double-quantum Hamiltonian based on a POST-C7 pulse sequence is used to recouple the homonuclear dipole-dipole interactions. Similar to the heteronuclear rotational echo double-resonance (REDOR) method, an analysis of the difference signal at short evolution times yields site-resolved summed squares of the dipole-dipole coupling constants.

NMR Spectroscopy

J. Ren, H. Eckert* — 12888–12891

A Homonuclear Rotational Echo Double-
Resonance Method for Measuring Site-
Resolved Distance Distributions in I = 1/2
Spin Pairs, Clusters, and Multispin
Systems

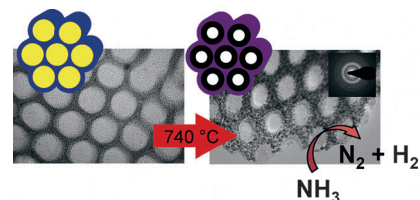
Ordered Carbides

T. Lunkenbein, D. Rosenthal, T. Otremba, F. Girgsdies, Z. Li, H. Sai, C. Bojer, G. Auffermann, U. Wiesner, J. Breu* 12892 – 12896



Access to Ordered Porous Molybdenum Oxycarbide/Carbon Nanocomposites

Hexagonally ordered mesoporous molybdenum oxycarbide/carbon (MoC/C) nanocomposites were directly accessed by heat treatment of mesostructured poly-(butadiene-*block*-2-vinylpyridine) (PB-*b*-P2VP) and molybdophosphoric acid. PB-*b*-P2VP serves as structure-directing agent and as carbon source. The high specific surface area obtained for the nanocomposites renders the materials interesting for potential applications, such as in the catalytic decomposition of NH_3 .



Supporting information is available on www.angewandte.org (see article for access details).



A video clip is available as Supporting Information on www.angewandte.org (see article for access details).



This article is available online free of charge (Open Access).

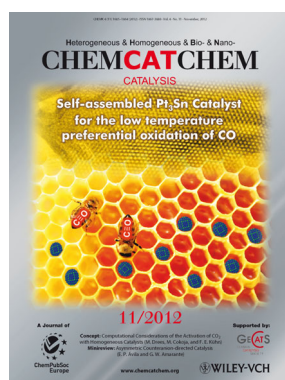


This article is accompanied by a cover picture (front or back cover, and inside or outside).

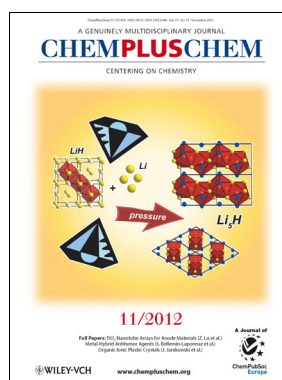
Check out these journals:



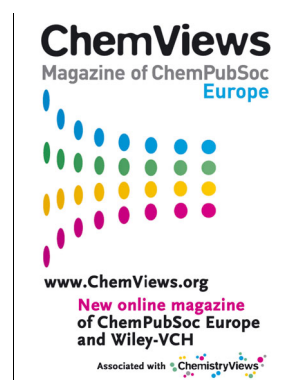
www.chemasianj.org



www.chemcatchem.org



www.chempluschem.org



www.chemviews.org